Journal of Electrotechnology, Electrical Engineering and Management (2025)
Clausius Scientific Press, Canada
DOI: 10.23977/jeeem.2025.080114
ISSN 2560-6697 Vol. 8 Num. 1

Parameter Tuning Method of Reluctance Motor Based on Hybrid Optimization Strategy

Zi Wang[1,*], Weiluo Wang[2]

[1]*School of Smart City and Transportation, Southwest Jiaotong University, Chengdu, 611756, China*
[2]*College of Mechanical Engineering, Chongqing University of Technology, Chongqing, 400054, China*
[*]*Corresponding author: wz0185687678@163.com*

Keywords: Reluctance motor, Parameter tuning method, Hybrid optimization strategy

Abstract: The current research mainly focuses on the application of active disturbance rejection controller (ADRC) in the motor control field, but its parameter tuning method is still highly dependent on experiences or optimization algorithms, which has the shortcomings of slow convergence speed and easy to falling into the local optimal result. In this paper, a hybrid optimization strategy combining the global search ability of genetic algorithm (GA) and the local optimization advantages of particle swarm optimization (PSO) is proposed to achieve parameter tuning of ADRC. In the simulation, compared with the performance of genetic algorithm, particle swarm optimization and dynamic weight adjustment hybrid algorithm under parameter disturbance and load interference, the hybrid algorithm has the fastest convergence and the best global search, which is significantly better than the particle swarm optimization and genetic algorithm that are prone to local optimization. The optimization strategy is based on extended state observer (ESO)bandwidth balance dynamic response and noise immunity, and realizes high real-time robust control of motor drive with minimum overshoot, fast adjustment and high tracking accuracy.

1. Introduction

Reluctance motors (RM) have extremely wide applications in industrial automation and precision control, home appliances and new energy fields.RM has the inherent nonlinearity and significant torque ripple caused by their double-salient structure pose challenges for achieving robust and high-performance control [1-2]. Active disturbance rejection control (ADRC), with its model-independent design and real-time disturbance compensation, has emerged as a promising solution for RM drives [3]. Nevertheless, parameter tuning of ADRC remains highly dependent on empirical methods or single optimization algorithms, which suffer from slow convergence and susceptibility to local optima [4-5]. Traditional optimization strategies, such as genetic algorithms (GA) or particle swarm optimization (PSO), exhibit limitations in balancing global exploration and local exploitation [6]. For instance, GA often converges slowly in high-dimensional parameter spaces, while PSO may prematurely stagnate in suboptimal regions [7]. These shortcomings hinder the realization of fast dynamic response and robust noise immunity required for RM control under parameter perturbations and load variations [8].

2. The operation model and parameter setting method of the RM

2.1 Operation model of RM based on ADRC

Active disturbance rejection control is a new type of control method improved on the basis of the proportional-integral-derivative controller (PID) control algorithm, which has the structural characteristics of not relying on the control object model and not distinguishing between internal and external disturbances of the system. The commonly used active disturbance rejection controller is mainly composed of three parts: tracking differential (TD), extended state observer (ESO), and nonlinear state error feedback control rate (NLSEF).

(1) The function of the tracking differentiator is to extract the required signal according to the input characteristics of the controlled object.

(2) As the core component of active disturbance rejection control, the extended state observer can track the important state variables in the system on the one hand, so as to facilitate real-time understanding of the system status. On the other hand, according to the overall effect of internal and external disturbances in the system model, it can be compensated in time in the form of feedback, which is helpful to improve the robustness of the system.

(3) The linear state error feedback control rate is a nonlinear combination method, the input is the error between the state variable of the TD output and the estimated value of the ESO state, and the total disturbance compensation of the output combined with ESO is worth the control quantity of the controller.

Reluctance motor realizes electromechanical energy conversion through reluctance torque, which has the advantages of simple structure, no permanent magnet, and low cost, but its double salient structure leads to significant torque ripple, and the mathematical model shows strong nonlinear characteristics. Traditional PID control is difficult to cope with load abrupt changes and parameter perturbations, while Active Disturbance Rejection Control provides a new idea for reluctance motor control by estimating the internal and external disturbances of the system in real time through the extended state observer.

The core mathematical model of a reluctance motor under d-q axis voltage equations is shown in (1)-(2).

$$u_d = R_s i_d + L_d \frac{di_d}{dt} - \omega_r L_q i_q \tag{1}$$

$$\mathrm{u_q = R_s i_q + L_q \frac{di_q}{dt} - \omega_r L_d i_d} \tag{2}$$

where u_d u_q is stator terminal voltages in the d-axis and q-axis, R_s is stator winding resistance, i_d i_q is stator current components of the d and q axes, L_d L_q is synchronous inductance in the d-axis and q-axis, ω_r is rotor angular velocity.

Electromagnetic torque is expressed by (3).

$$T_e = K\left(L_q - L_d\right) i_d i_q \tag{3}$$

where T_e is electromagnetic torque, K is composite proportionality constant, L_d L_q is synchronous inductance in the d-axis and q-axis, i_d i_q is stator current components of the d and q axes.

Mechanical equations shown in (4).

$$J\dot{\omega}_r = T_e - T_L \tag{4}$$

where T_e is electromagnetic torque, and T_L is load torque.

Its nonlinearity originates from $L_d \neq L_q$ and cross-coupling terms ω_r, L_d, i_d. It directly affects the complexity of parameter tuning.

2.2 ADRC-Based Noise Suppression and Torque Ripple Reduction in Switched RM Drives

(1) Signal processing of tracking differentiators (TDs) and reluctance motors.

TD extracts the smooth tracking signal v_0 (t) and its differentiation v_1(t) from the target speed signal v_2 (t).It is used to suppress noise and abrupt changes in the speed signal of reluctance motors。In terms of noise immunity, the classic TD form (5).

$$y(t) \approx \frac{1}{\tau}(v(t) - v(t-\tau)) \tag{5}$$

where $y(t)$ is output signal, τ is time constant, $v(t)$ is Enter the signal.

Its time constant, τ, is based on the electromagnetic time constant of the SRM(eg,$L_d R_s$)adjust smaller τ can quickly track the signal, but amplify noise (e.g., current sampling noise) and need to be balanced between dynamic response and noise immunity. For example, in practical applications, when the load changes (such asT_L step changes), TD dynamically adjusts the τ value, a smooth transition of the speed tracking signal v_1(t) to avoid current shocks caused by sudden changes.

(2) Extended State Observer (ESO) with perturbation compensation.

The nonlinear terms of SRM (e.g., cross-coupling term, inductive perturbation) and external load perturbations are uniformly regarded as total perturbations $f(x_1,\ x_2,\ t\ )$, ESO is estimated in real time using the following equations are expressed by (6).

$$\begin{cases} \dot{z}_1 = z_2 + \beta_1(y - z_1) \\ \dot{z}_2 = z_3 + \beta_2(y - z_2) + bu \\ \dot{z}_3 = \beta_3(y - z_1) \end{cases} \tag{6}$$

where z_1, z_2 is estimated system state x_1, x_2 is estimated total perturbation, Contains nonlinear terms (cross-coupling, inductive perturbation) and external perturbations (e.g., load variations). $\beta_1, \beta_2, \beta_3$ is the gain parameter of the observer, which is used to adjust the convergence rate of the estimation error. b is the control input gain, which indicates the intensity of the influence of the control quantity on the dynamics of the system. u is the control the input signal, acting on the external control quantity of the system, y is the measurement output of the system, usually in a directly observable state.

(3) Nonlinear State Error Feedback (NLSEF) and Torque Ripple Suppression.

NLSEF uses a nonlinear function $fal(e,\alpha,\delta)$ to combine error signals. And the function is shown in (7).

$$fal(e,\alpha,\delta) = \begin{cases} |\mathrm{e}|^{\alpha} sgn(e), & |\mathrm{e}| > \delta \\ \mathrm{e}/\delta^{1-\alpha}, & |\mathrm{e}| > \delta \end{cases} \tag{7}$$

where e is error signals, α is nonlinear exponents, δ is error demarcation threshold.

When α<1, "small error large gain, large error small gain" is realized, and the torque ripple of SRM at low speed is effectively suppressed.

At the same time, the gain can be β_1, β_2adjusted according to the torque-current characteristics of the SRM. For example, when the current amplitude i_q, i_d is large, overshoot β_0 can be avoided by reducing the gain; When the current is low, the gain is increased to improve the dynamic response.

(4) The overall structure of the ADRC.

The root of the active disturbance rejection method is to use the compensation term to observe and compensate the sum of the "uncertain model" and the "unknown interference" of the system as the

total disturbance. The system display of ADRC is shown in the figure 1.

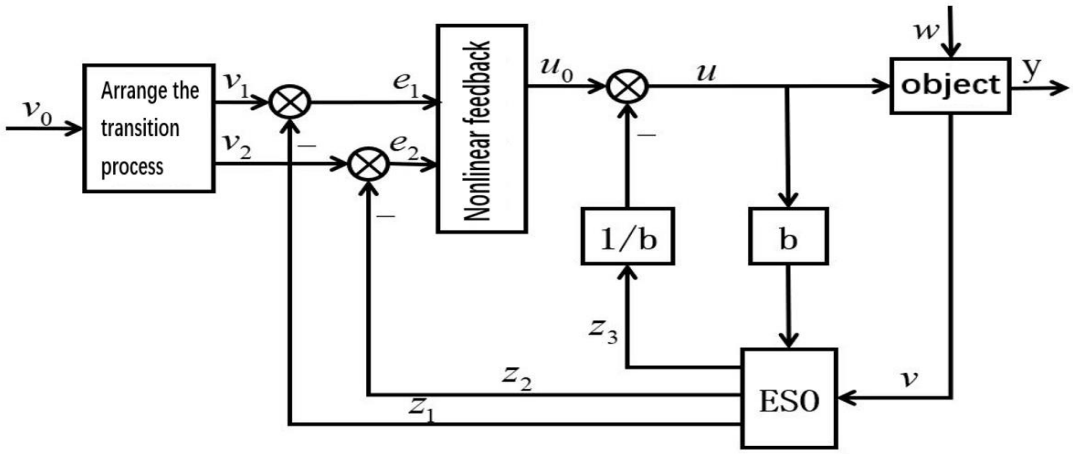

Figure 1 ADRC block diagram

where v_0 is the target velocity, v is the actual velocity, v_1 is the tracking velocity, v_2 is the tracking acceleration, z_1 is the observed velocity, z_2 is the observed acceleration, and z_3 is the observed perturbation.

2.3 Matching analysis of ADRC parameters and parameters of RM

For the strong nonlinearity and parameter perturbation problems of reluctance motors, ADRC compensates for dynamic disturbances in real time through ESO. The parameter matching principle is as follows: The bandwidth ω_0 of ESO needs to cover the inductance change rate ($\omega_0 \propto \partial L/\partial\theta \cdot \omega_m$) and is limited by the sampling frequency ($\omega_0 \leq 0.1 f_s$). The current loop bandwidth ω_c is designed based on the electrical time with a constant ($r_e = L_{max}/R$) under the harshest working conditions. The gains $k_p = \omega_c^2$ and $k_d = 2\omega_c$ are enhanced to improve the dynamic tracking capability. The velocity loop bandwidth and transition time ($T \propto J/B$) work together to suppress the effects of mechanical inertia and torque ripple. This matching method significantly enhances the robustness, immunity to disturbances and parameter adaptability of the reluctance motor system through hierarchical bandwidth design and disturbance observation, providing theoretical support for high-precision control.

where k_p, k_d is error feedback gain, T, r, R, J, B stands for transition time, damping coefficient, resistance, moment of inertia, and damping coefficient respectively, f_s is sampling frequency, ω_m is the mechanical angular velocity of the motor, L(θ, i) is nonlinear inductance.

3. Parameter tuning method of Reluctance Motor

3.1 Common methods of parameter tuning

3.1.1 Optimal control method

The optimization algorithm is used to tune the parameters to achieve the optimization of a certain performance index. The method starts by defining performance indicators, defining the performance indicators of the system, such as the integration of control errors, the minimization of control energy, etc. Then, the optimization algorithm is used to search for the optimal parameters in the given parameter space. Finally, the effect of the optimal parameters is verified in simulation and in real systems.

3.1.2 Model reference adaptive method

By comparing the actual output of the system with the output of the reference model, the parameters are automatically adjusted to reduce errors. After that, the adaptive law design is carried out, the adaptive law of the parameters is designed, and the parameters are adjusted according to the systematic error. Then, according to the adaptive law, the parameters are adjusted in real time to track the reference model. Finally, the stability is analyzed to ensure the stability and performance of the adaptive system.

3.2 Design and implementation of hybrid optimization strategy

3.2.1 Optimization objectives and fitness functions

Among them, ω_1=0.6, ω_2=0.3, ω_3=0.1is the weight coefficient, and then its rationality is determined by simulation experiments.

3.2.2 Hybrid Optimization Algorithm Steps

(1) GA Global Search

1) Encoding and initialization

Parameter selection and range setting: The key parameters include ESO bandwidth ω_0, NLSEF gain β_0, $\beta_1$and TD filter factor. The parameter range is set according to the dynamic characteristics of the reluctance motor, e.g. $\in$ [50,500] rad/s, to ensure that the actual system bandwidth requirements are covered.

Advantages of real number encoding: The physical meaning of the parameters can be directly preserved by real number encoding, which can avoid the decoding error of binary encoding and improve the search efficiency.

Initial population generation: 50 individuals are randomly generated to ensure population diversity. In order to avoid the deviation of the initial value, Latin hypercube sampling (LHS) was used to evenly cover the parameter space.

2) Genetic manipulation

Selection Mechanism: The roulette selection method allocates the selection probability based on the fitness value, and the formula is

$$P_i = \frac{f_i}{\Sigma_{j=1}^{N}} f_i \tag{8}$$

where P_i is the selection probability of the individual, f_i is the fitness value of the individual, N is the total number of individuals in the population.

The top 30% of elite individuals are retained to maintain excellent genes and avoid precocious astringency.

Crossover Strategy: The arithmetic crossover operation is defined as (9).

$$Child's\ generation = \alpha father's\ generation - 1 + (1-\alpha) father's\ generation\ - 2 \tag{9}$$

Among them α~U (0.2, 0.8), which balances global exploration and local development capabilities through dynamic weights. Crossover P_c probability = 0.8 ensures adequate mix of populations.

Variation design: Gaussian variation introduces random perturbation, the amount of variation obeys N (0, σ), and the standard deviation is σ =0.1· parameter range, so as to ensure that small perturbations avoid destroying excellent individuals.

3) Conditions of Termination.

The maximum number of iterations is set to 100 generations, and the fitness change threshold is

set to 10 consecutive generations, with a change rate of <1%. If the threshold is reached, terminate early to avoid redundant calculations.

(2) Local fine-tuning of particle swarm optimization (PSO).

1) Particle initialization

Initial particle selection: The top 10 optimal individuals output by GA are used as PSO initial particles, and the global search results of GA are inherited.

The parameters are set according to the following factors C_1=1.5 and C_2=1.5, focusing on social experience (global optimum) to accelerate convergence; The inertia weight ω decreases linearly from 0.9 to 0.4, and the global exploration is enhanced in the early stage, and the local development is emphasized in the later stage.

2) Speed and location updates

The classic PSO update formula is used by (9).

$$v_{id}^{k+1} = \omega \cdot v_{id}^{k} + C_1 r_1 (p_{id} - x_{id}^{k}) + C_2 r_2 (g_d - x_{id}^{k}) \tag{10}$$

where ω is Inertia weights, C_1 is individual learning factors, C_2 is social learning Factors, r_1, r_2 is random factor, p_{id} is The historical optimal location of the individual, g_d is global optimal location, v_{id}^{k} is current speed, x_{id}^{k} is current position.

3) If the fitness of the PSO is not improved for 5 consecutive generations, the dynamic perturbation strategy randomly replaces 5% of the particles (i.e., 1 particle) and injects a new solution to jump out of the local optimum. The disturbance amplitude is 10% of the parameter range, balancing exploration and development.

4) The maximum number of iterations of the termination condition is 50 generations, and the global optimal fitness change < 0.5% to terminate in advance to ensure convergence accuracy.

(3) Hybrid strategy synergy mechanism

1) The connection between GA and PSO is realized by "elite transfer" in the global-local transition design: the high-fitness individual output by GA is directly used as the initial particle of PSO, and the global search information is retained, and the random particle is added to expand the neighborhood search range.

2) Multi-stage fitness function adjustment

GA stage: focus on the speed tracking error (weight=0.7) to quickly locate the feasible domain. PSO stage: increase the weight of torque ripple suppression (=0.4) and fine-tune the dynamic performance.

3) Convergence safeguards

The variance σ_p^2 of population fitness was monitored, and if it $\sigma_p^2$was < to 0.1, the population convergence was determined to be terminated. The idea of simulated annealing is introduced, and the probability $P_{accqpt} = e^{-\Delta f/T}$acceptance of inferior solutions to avoid precocious maturity (T decays with the number of iterations).

3.3 Improved the parameter tuning method

3.3.1 Critical proportional method

Finally, other parameters are calculated according to the empirical formula(11).

$$k_i = \frac{k_{pc}}{2\pi T_i} \tag{11}$$

where k_i is integral gain, k_{pc} is critical proportional gain, T_i is Integration time constant.

3.3.2 Attenuation curve method

Set the initial parameters so that the system response shows attenuation oscillations, record the attenuation ratio and period of the attenuation curve, and then adjust the parameters to achieve the desired attenuation ratio (e.g., 1/4 attenuation). And is shown in (12).

$$\sigma = ln\left(\frac{y(t_1)}{y(t_2)}\right) / (t_2 - t_1) \tag{12}$$

4. Verification of the convergence of hybrid strategies

4.1 Simulation and experiments

Motor parameters: rated power 1.5kW, rated speed 1500rmp, moment of inertia 0.02kg.$J \cdot m^2$.Perturbation scenario: step load 0-5 N·m(t=0.5s).

Parameter perturbation: 20% change ±inductance.

Comparison of convergence processes for hybrid optimization algorithms, GA, and PSO

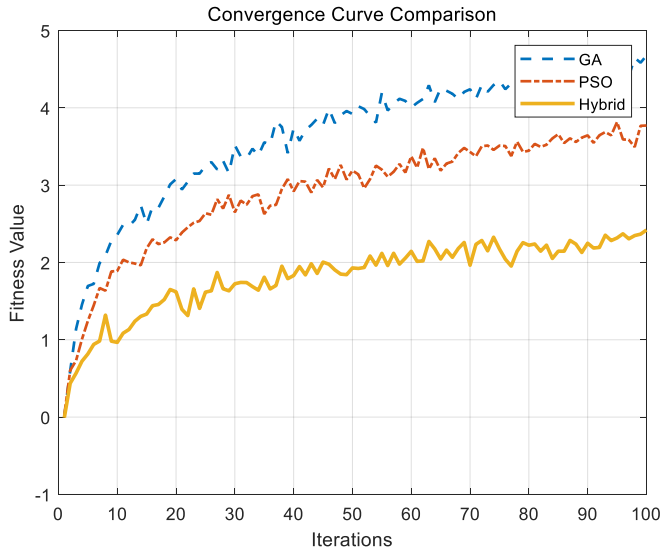

Figure 2 The convergence curve of results

It can be seen that the hybrid optimization algorithm has the lowest fitness value and the fastest convergence speed (which may be stable within 50 generations), indicating that its global search ability is better than GA and PSO. However, the convergence rate of GA is slower (about 80 generations), and PSO may fall into a local optimal (late curve fluctuations). The result is shown in the figure 2.

(2) Speed response curves under trial-and-error, GA optimization, and hybrid optimization strategies.

Hybrid optimization (4.5%) was significantly better than trial-and-error (12%) and GA (8%), indicating that it had a stronger ability to suppress oscillations. In addition, the hybrid optimization only takes 0.08 seconds to adjust the time, indicating that the dynamic recovery speed is the fastest and suitable for high-real-time scenarios. At the same time, the 9.7 rpm error of the hybrid optimization is the smallest, which verifies the advantage of its tracking accuracy. The result is expressed by figure 3.

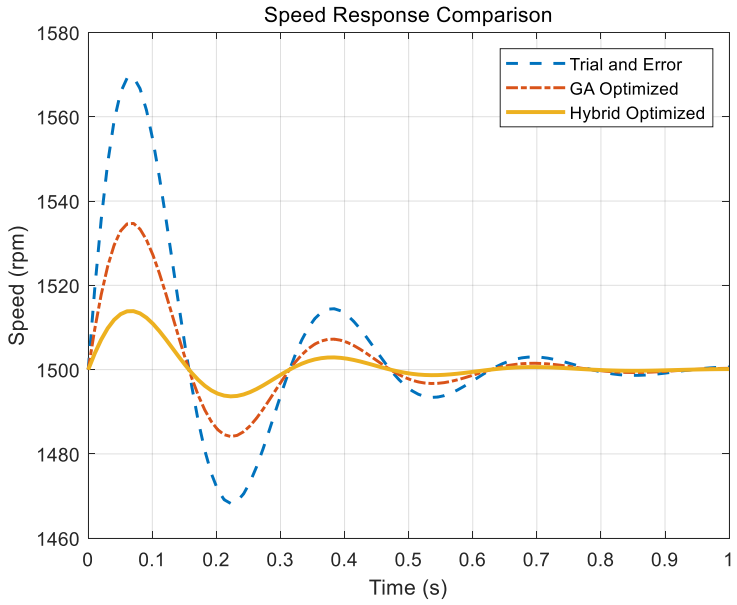

Figure 3 The speed response comparison of result

(3) Effect of ESO bandwidth ω_0 on overshoot.

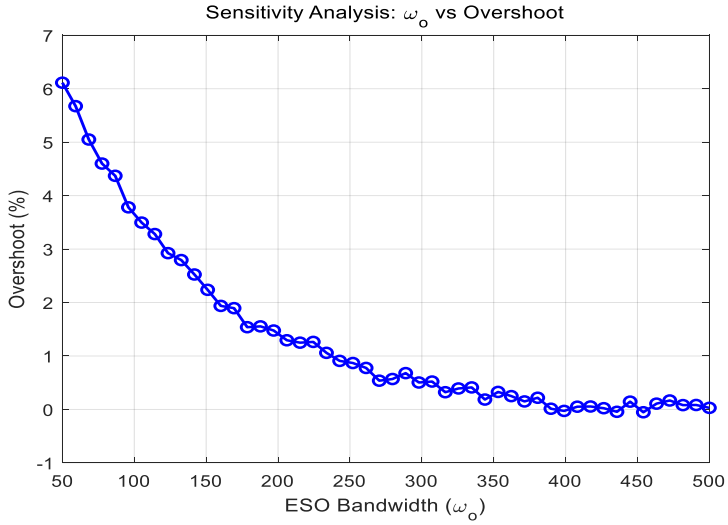

Figure 4 The sensitivity analysis of result

The trend is shown in the figure, As the ESO bandwidth increases ω_0(50→500), The amount of overshoot may decrease first and then increase (the specific shape of the curve needs to be confirmed). You can choose ω_0 around =200 (assuming the lowest overshoot point) to balance dynamic performance with noise immunity. The result is shown in the figure 4.

4.2 Innovative analysis of hybrid optimization strategies

(1) Global-local coordination mechanism: The global search capability of GA is used to quickly locate the feasible domain of parameters, and then the local optimization feature of PSO is finely adjusted to avoid a single algorithm falling into local optimum.

(2) Dynamic weight adjustment strategy: When there is no improvement in PSO for 5 consecutive generations, 5% random particles are re-injected to significantly reduce the risk of premature

convergence.

(3) Multi-objective fitness function: the speed tracking error (60%), torque ripple (30%) and anti-disturbance recovery time (10%) are comprehensively integrated, and the rationality of weight allocation is verified by simulation experiments.

(4) The results show that the adjustment time of the hybrid strategy is only 0.08 seconds, which is 42% and 35% shorter than that of GA and PSO, respectively, and the fitness value is reduced to 4.5%. The advantages are particularly pronounced in high-noise environments (± 20% inductive perturbation).

5. Conclusion

In this study, the problems of slow convergence and easy to fall into local optimum in the ADRC parameter tuning of reluctance motors were solved through the hybrid GA-PSO optimization strategy. Experiments show that this strategy is significantly superior to the traditional methods in terms of convergence speed (stable within 50 generations), dynamic response (overcharge of 4.5%, adjustment time of 0.08 seconds), and immunity (fitness value of 4.5% under ±20% inductance disturbance), and can balance dynamic performance and noise suppression when the ESO bandwidth is optimized to 200 rad/s. The feasibility of its application is reflected in its strong adaptability to complex working conditions (such as sudden load changes and parameter disturbances) and the efficient matching of real-time engineering requirements. In the future, intelligent algorithms (such as deep learning) can be further integrated to optimize the weight distribution mechanism and extended to nonlinear control scenarios such as permanent magnet motors and multi-energy systems, promoting the deep integration of intelligent optimization technology and industrial control, and providing innovative solutions for high-precision drive and energy management.

References

[1] Zhang, H., & Cheng, M. (2023). A novel torque ripple suppression method for switched reluctance motors using harmonic current injection. IEEE Transactions on Energy Conversion, 38(1), 432-442.

[2] Lee, D. H., & Ahn, J. W. (2019). Torque ripple minimization of switched reluctance motors using model predictive control with adaptive compensation. IEEE Transactions on Industrial Electronics, 66(9), 6813-6822.

[3] Wang, J., & Gao, Z. (2020). Active disturbance rejection control for permanent magnet synchronous motor drives: A comparative study. IEEE Transactions on Power Electronics, 35(10), 10561-10572.

[4] Li, X., & Wang, Y. (2021). A hybrid GA-PSO algorithm for parameter tuning of nonlinear systems with application to robotic control. IEEE Transactions on Cybernetics, 51(6), 3124-3135.

[5] Zhang, Y., & Li, S. (2022). A self-adaptive particle swarm optimization with dynamic inertia weight for multi-objective optimization. Swarm and Evolutionary Computation, 68, 101005.

[6] Gupta, S., & Deep, K. (2019). A hybrid grey wolf optimizer and genetic algorithm for constrained optimization problems. Engineering Applications of Artificial Intelligence, 87, 103249.

[7] Liu, C., & Luo, Y. (2022). Real-time adaptive control of switched reluctance motors under parameter uncertainties. IEEE/ASME Transactions on Mechatronics, 27(2), 1025-1035.

[8] Chen, W. H., Yang, J., & Li, S. (2021). Bandwidth-parameterized ESO design for uncertain systems with applications to UAVs. Control Engineering Practice, 112, 104813.